ENCYCLOPEDIA OF PHYSICAL SCIENCE & TECHNOLOGY
R. A. Meyers Ed., Academic Press, Vol. 15, pp. 237-256, 2001.

SOLAR THERMOCHEMICAL PROCESS TECHNOLOGY

Aldo Steinfeld
Institute of Energy Technology
Department of Mechanical and Process Engineering
ETH – Swiss Federal Institute of Technology
CH-8092 Zurich, Switzerland

Robert Palumbo
Laboratory for Solar Technology
Department of General Energy Research
Paul Scherrer Institute
CH-5232 Villigen, Switzerland

Outline:

Glossary

aperture – opening of a solar cavity-receiver

Carnot efficiency – the maximum efficiency for converting heat from a high-temperature thermal reservoir at T_H into work in a cyclic process and rejecting heat to a low-temperature thermal reservoir at T_L, given by $1\text{-}T_L/T_H$

CPC (Compound Parabolic Concentrator) – a non-imaging concentrating device that is usually positioned in tandem with the primary parabolic concentrating system for further augmentation the solar concentration ratio

detoxification – a process in which hazardous materials are decomposed to harmless and environmentally compatible compounds

endothermic – absorbs heat

exothermic – rejects heat

exergy efficiency (for a solar thermochemical process) – the efficiency for converting solar energy into chemical energy. It is given by the ratio of the maximum work (e.g., electrical work) that may be extracted from a solar fuel to the solar energy input for producing such a fuel

normal beam insolation – power flux of direct solar irradiation on a surface perpendicular to the sun rays

solar cavity-receiver – a well-insulated enclosure, with a small opening to let in concentrated solar energy, which approaches a blackbody absorber in its ability to capture solar energy

solar chemical heat pipe – concept for storing and transporting solar energy using a reversible endothermic reaction

solar concentration ratio – non-dimensional ratio of the solar flux intensity (e.g., in "suns") achieved after concentration to the normal insolation of incident beam

solar fuels – fuels produced with solar energy

solar thermochemical process – any endothermic process which uses concentrated solar energy as the source of high-temperature process heat

specular (mirror-like) - the angle between the incident ray and the normal to the surface equals the angle between the reflected ray and the normal to the surface

syngas – synthesis gas (a mixture of primarily hydrogen and carbon monoxide), which serves as the building block for a wide variety of synthetic fuels including Fischer-Tropsch type chemicals, hydrogen, ammonia, and methanol

water-splitting – chemical process or cycle aimed at obtaining hydrogen and oxygen from water

Nomenclature

$A_{aperture}$	area of reactor aperture
C	solar flux concentration ratio
I	normal beam insolation
Irr_{quench}	irreversibility associated with quenching
$Irr_{reactor}$	irreversibility associated with the solar reactor
$\dot{n}$	molar flow rate of reactant
$Q_{aperture}$	incoming solar power intercepted by the reactor aperture
Q_{FC}	heat rejected to the surroundings by an ideal fuel cell
Q_{quench}	heat rejected to the surroundings by the quenching process
$Q_{reactor,net}$	net power absorbed by the solar reactor
Q_{solar}	total solar power coming from the concentrator
T	nominal solar cavity-receiver temperature
$T_{stagnation}$	maximum temperature of a blackbody absorber
$T_{optimum}$	optimal temperature of the solar cavity-receiver for maximum $h_{exergy,ideal}$
W_{FC}	work output by an ideal fuel cell
a_{eff}	effective absorptance of the solar cavity-receiver
e_{eff}	effective emittance of the solar cavity-receiver
DG	Gibbs free energy change per mole of reactant
DH	enthalpy change per mole of reactant
DS	entropy change per mole of reactant
r	reflectivity
q	angle subtended by the sun at the earth's surface (approximately 0.0093 rad)
$h_{absorption}$	solar energy absorption efficiency
h_{Carnot}	efficiency of a Carnot heat engine operating between T_H and T_L
h_{exergy}	exergy efficiency
$h_{exergy,ideal}$	exergy efficiency of an ideal system
F_{rim}	rim angle of a parabolic concentrator
s	Stefan-Boltzmann constant (5.6705×10^{-8} $Wm^{-2}K^{-4}$)

I. INTRODUCTION

One of the most abundant resources on the surface of the earth is sunlight. Yet we do not typically think of this resource as the solution to any upcoming energy crisis or as the "fuel" that will bring clean air to our cities. We just cannot see ourselves driving into the local gasoline station and filling our cars up with sunlight. Perhaps it is for this reason that this resource does not capture our imagination as the ingredient that could help us deal with two of the most pressing problems that we will meet head-on in the 21st century, namely, the impending shortage of crude oil and environmental pollution. A number of scientists and engineers from around the world are intrigued by a rather staggering fact: using only 0.1% of the earth's land space with solar collectors that operate with a collection efficiency of merely 20%, one could gather more than enough energy to supply the current yearly energy needs of all the citizens of the planet. Furthermore, the solar energy reserve is essentially unlimited. No particular individual or government owns it. And its utilization is ecologically benign. Good enough reasons to expect increasing utilization of solar energy, if it were not for the following very serious drawbacks: solar radiation reaching the earth is very dilute (only about 1 kW per square meter), intermittent (available only during day-time), and unequally distributed over the surface of the earth (mostly between 30° north and 30° south latitude). Scientists ask themselves how can we get hold of solar energy such that it can be stored and transported from the sunny and uninhabited regions of the earth's sunbelt to the world's industrialized and populated centers outside the earth's sunbelt, where much of the energy is required?

This question has motivated the search for recipes that convert sunlight into a fuel that one can use to propel not only our cars but the entire world economy. In other words, these investigators are looking for processes (and reactors for conducting these processes) that can convert intermittent solar radiation falling in the deserts of the world into storable chemical energy, in the form of fuels, that can be transported to the population centers. Cars running on fuels produced from such a recipe would be, in fact, running on solar energy, even if it happens to be a rainy evening.

The means by which sunlight can be used to produce fuels for the 21st century can be found in the writings of two of the prominent scientists of the 19th century, Carnot and Gibbs. They created the discipline of thermodynamics, which is the study of how energy can be converted from one form to another, for example, from solar to chemical energy. In very simple terms, thermodynamics tells us that the higher the temperature at which we supply solar energy to our process, the more creative we can be with what comes out as a final product. For example, if we use sunlight in a typical flat-plate solar collector, we can produce warm water that could be used for taking baths or supplying space heat. Although this type of device can make a great deal of sense for certain local conditions, it will not enable solar energy collected in Australia to be transported to Japan. But if we supply solar energy to a chemical reactor at very high temperatures near 2300 K, we open up the possibility for such a feat: solar energy collected in Australia can heat homes, supply electricity, propel cars, and more ... in Tokyo.

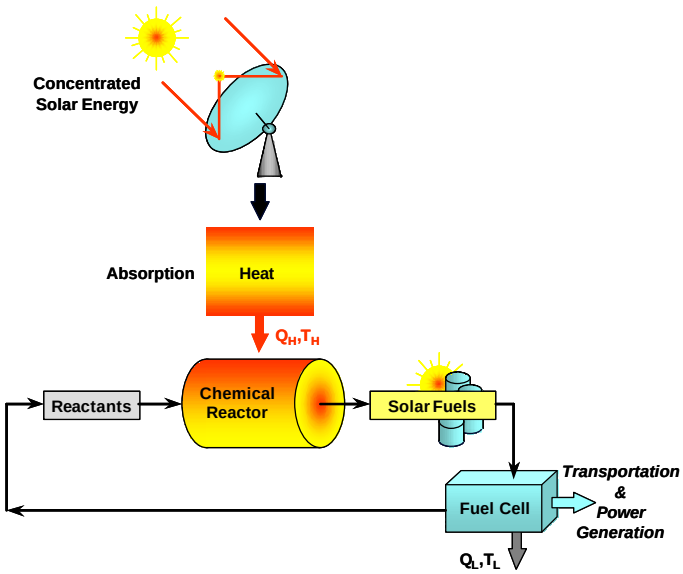

Figure 1. Schematic of solar energy conversion into solar fuels. Concentrated solar radiation is used as the energy source for high-temperature process heat to drive chemical reactions towards the production of storable and transportable fuels.

Figure 1 illustrates the basic idea. If we concentrate the diluted sunlight over a small area with the help of parabolic mirrors and then capture that radiative energy with the help of suitable receivers, we would be able to obtain heat at high temperatures for driving a chemical transformation and producing a storable and transportable fuel. Regardless of the nature of the fuel, the theoretical maximum efficiency of such an energy-conversion process is limited by the Carnot efficiency of an equivalent heat engine. With the sun's surface as a 5800 K thermal reservoir and the earth as the thermal sink, 95% of the solar energy could, in principle, be converted into the chemical energy of fuels. It is up to us to design

and develop the technology that approaches this limit.

This article develops some of the underlying science and describes some of the latest technological developments for achieving this goal. The reader is first introduced to the principles of solar energy concentration and to the thermodynamics of solar thermochemical conversion. State of the art reactors are described as well as the most promising solar thermochemical processes.

II. PRINCIPLES OF SOLAR ENERGY CONCENTRATION

The conventional method for concentrating solar energy, i.e. collecting solar energy over some large area and delivering it to a smaller one, is by parabolic-shaped mirrors. A parabola focuses rays parallel to its axis into its focal point. However, sun rays are not parallel. To a good approximation they can be assumed to originate at a disk which subtends the angle q=0.0093 radian. When a perfectly specular reflective paraboloid of focal length f and rim angle F_{rim} is aligned to the sun, reflection of the rays at the focal plane forms a circular image centered at the focal point (shown in Fig. 2). It has the diameter,

$$d = \frac{f \times q}{\cos F_{rim}(1+\cos F_{rim})} \qquad (1)$$

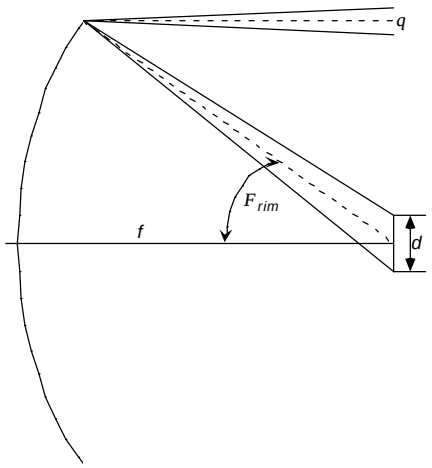

Figure. 2. Concentration of sunlight by a parabolic dish of focal length f and rim angle F_{rim}. When the dish is aligned toward the sun, reflection of sun rays at the focal plane forms a circular image centered at the focus of diameter d.

On this circle, the radiation flux intensity is maximum and uniform in the paraxial solar image (the "hot spot"). It decreases for diameters larger than $f \times q$ as a result of forming elliptical images. The theoretical concentration ratio C at the hot spot is defined as the ratio of the radiation intensity on the hot spot to the normal beam insolation, and is approximately

$$C \approx \frac{4}{q^2} \sin^2 F_{rim} \qquad (2)$$

For example, for a rim angle of 45°, the theoretical peak-concentration ratio exceeds 23,000 suns, where 1 sun refers to the normal beam insolation of 1 kW/m^2. The thermodynamic limit for solar concentration is given by the factor $\sin^{-2} q \approx 46{,}000$ suns. In practice, the achievable concentration ratios are much smaller. Losses in power and concentration are due to geometrical imperfections (such as a segmented approximation to the exact parabolic profile, facet misalignments, structural bending and deformations), optical imperfections (such as poor reflectivity and specularity of the mirrors and glass absorption), shading effects (such as shading caused by the receiver and the non-reflective space or frame around each mirror facet), and tracking imperfections.

Three main optical configurations based on parabolic-shaped mirrors are commercially available for large-scale collection and concentration of solar energy. These are the trough, tower, and dish systems. These three systems are shown schematically in Fig. 3 (Tyner *et al.*, 1999). Trough systems use linear, 2-dimensional, parabolic mirrors to focus sunlight onto a solar tubular receiver positioned along their focal line. Tower systems use a field of heliostats (two-axis tracking parabolic mirrors) that focus the sun rays onto a solar receiver mounted on top of a centrally located tower. Dish systems use paraboloidal mirrors to focus sunlight on a solar receiver positioned at their focus. The total amount of power collected by any of these systems is proportional to the projected area of the mirrors. Their arrangement depends mainly on the concentrating system selected and on the site latitude. Trough systems are usually arranged in rows along the east-west direction and track the sun along the south-north direction, as is the case for the SEGS plant at Kramer Junction, USA. Tower systems, which are also referred to as central-receiver systems, may have instead a circular field of heliostats with a centred receiver on top of the tower, as for the Solar-Two plant at Barstow, USA, or may also have an asymmetric field, as for the south-facing plant at Plataforma Solar de Almeria, Spain. A recently developed Cassegrain optical

configuration for the tower system at the Weizmann Institute of Sciences, Israel, makes use of a hyperboloidal reflector at the top of the tower to re-direct sunlight to a receiver located on the ground level (Yogev, 1998).

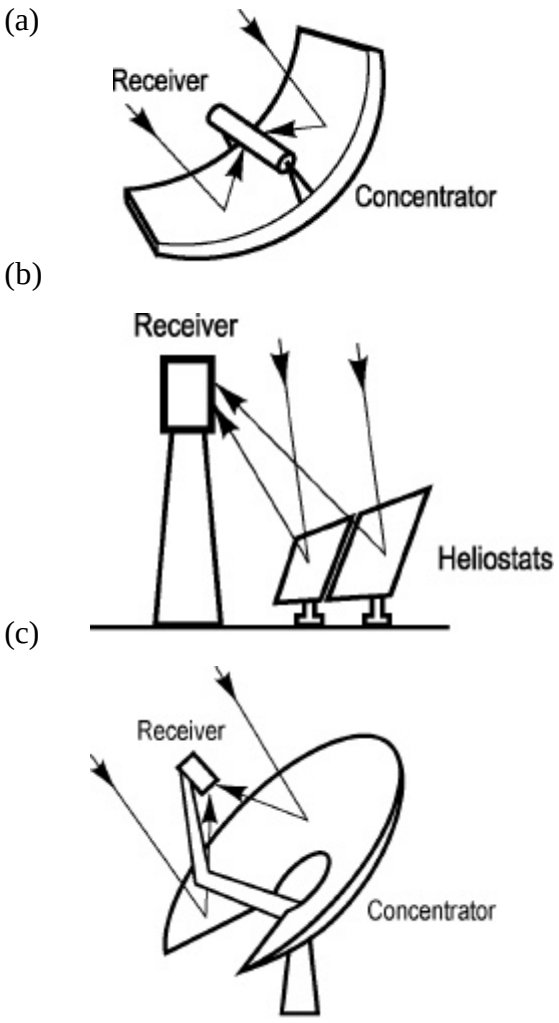

Figure 3. Schematic of the three main optical configurations for large-scale collection and concentration of solar energy: (a) the trough system, (b) the tower system, and (c) the dish system.

The solar flux concentration ratio C typically obtained at the focal plane varies between 30-100 suns for trough systems, 500-5,000 suns for tower systems, and 1000-10,000 for dish systems. Higher concentration ratios imply lower heat losses from smaller receivers and, consequently, higher attainable temperatures at the receiver. To some extent, the flux concentration can be further augmented with the help of non-imaging secondary concentrators, e.g., a compound parabolic concentrator, which is usually referred to as CPC (Welford and Winston, 1989). They are positioned in tandem with the primary concentrating systems. Figure 4 shows a schematic of a 2-dimensional CPC that can be applied to primary concentrating trough systems, and also a 3-dimensional CPC that can be applied to primary concentrating tower and dish systems. With such an arrangement, the power flux concentration can be increased by a factor $r\,(\sin F_{rim})^{-1}$ for 2D-CPC and by $r\,(\sin F_{rim})^{-2}$ for 3D-CPC, where F_{rim} is the rim angle of the primary concentrating system and r is the inner wall total hemispherical reflectance of the CPC. Other geometries for non-imaging concentrators based on total internal reflection of a dielectric-filled CPC have also been developed (Welford and Winston, 1989).

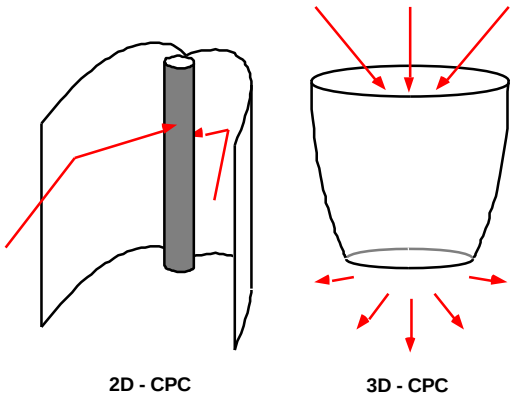

Figure 4. Schematic of a 2-D and 3-D compound parabolic concentrator (CPC). CPCs have specular reflective inner walls and can be used to augment the solar flux concentration of the primary concentrator. The arrows represent concentrated solar radiation arriving from the primary concentrator (from trough systems for the 2D-CPC and from tower or dish systems for the 3-D CPC).

Solar furnaces are concentrating facilities in which high-flux solar intensities are usually obtained at a fixed location inside a housed laboratory. They are experimental platforms for conducting research with high radiation fluxes and at high temperatures. The traditional design consists of using a sun-tracking, flat heliostat on-axis with a stationary primary paraboloidal concentrator (Haueter *et al.*, 1999); off-axis configurations have also been designed. A recent survey of solar furnace installations (SolarPACES, 1996) lists the test facilities presently in operation.

The solar concentrating systems described have been proven to be technically feasible in large-scale experimental demonstrations aimed mainly at the production of solar thermal electricity in which a working fluid (typically air, water, helium, sodium, or molten salt) is solar-heated and further used in traditional Rankine, Brayton, and Stirling cycles (Tyner *et al.*, 1999). Solar thermochemical applications, although not developed as far as solar thermal electricity generation, will make use of the same solar concentrating technology.

III. THERMODYNAMICS OF SOLAR THERMOCHEMICAL CONVERSION

Because thermodynamics is the science that describes the conversion of one form of energy into another form, it is germane to the field of *Solar Thermochemistry*. Solar thermochemical processes convert radiant energy into chemical energy. The two fundamental thermodynamic laws that give practical information with regard to any solar thermochemical process are the 1st and 2nd laws. Using the 1st law, one establishes the minimum amount of solar energy required to produce a particular fuel or chemical species. The 2nd law indicates, among other things, whether or not the chosen path for producing the fuel is physically possible. Both types of information are required for a process designer.

We consider as an example a generic solar process in which one wishes to effect the following chemical transformation:

$$reactants \rightarrow products\,. \qquad (3)$$

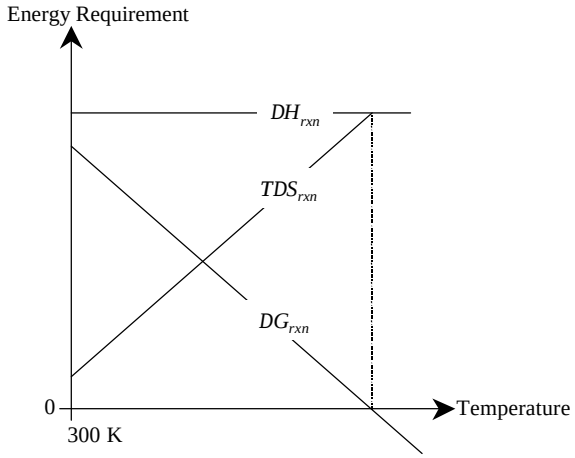

Figure 5. Variations of DH_{rxn}, DG_{rxn}, and TDS_{rxn} with temperature for a generic solar chemical reaction. DH_{rxn} is the total energy required to effect the transformation. DG_{rxn} is the portion of energy that must be supplied as high-quality energy in the form of work, for example, in the form of electrical work. The remainder TDS_{rxn} is the amount of energy that can be supplied as process heat for the completely reversible process in the form of solar thermal energy.

Figure 5 shows the energy requirements to effect this transformation as a function of temperature. The total energy required is the enthalpy change DH_{rxn} for the reaction. Of this total, an amount of energy equal to the Gibbs free energy for the reaction, DG_{rxn}, must be supplied as high-quality energy in the form of work, for example in the form of electric work. The remainder, TDS_{rxn}, is the amount of energy that can be supplied as process heat for the completely reversible process in the form of solar thermal energy. DG_{rxn} decreases with temperature. Consequently, the ratio of work (e.g., electrical energy) to thermal energy, DG_{rxn}/TDS_{rxn} , decreases as the temperature is increased. At temperatures for which $DG_{rxn} \leq 0$, the reaction proceeds spontaneously to the right when supplying only solar process heat.

The 1st law is also applied to calculate the solar energy absorption efficiency of a solar reactor, $h_{absorption}$. It is defined as the net rate at which energy is being absorbed divided by the solar power coming from the concentrator. Solar reactors for highly concentrated solar systems usually feature the use of a cavity-receiver type configuration, i.e. a well-insulated enclosure with a small opening (the *aperture*) to let in concentrated solar radiation. At temperatures above about 1000 K, the net power absorbed is diminished mostly by radiative losses through the aperture. For a perfectly insulated cavity-receiver (no convection or conduction heat losses), it is given by (Fletcher and Moen, 1977)

$$h_{absorption} = \frac{a_{eff} Q_{aperture} - e_{eff} A_{aperture} s T^4}{Q_{solar}} \qquad (4)$$

where Q_{solar} is the total power coming from the concentrator, $Q_{aperture}$ the amount intercepted by the aperture of area $A_{aperture}$, a_{eff} and e_{eff} are the effective absorptance and emittance of the solar cavity-receiver, respectively, T is the nominal cavity-receiver temperature, and s the Stefan-Boltzmann constant. The first term in the numerator denotes the total power absorbed and the second term denotes the re-radiation losses Q_{rerad}. Their difference yields the net power absorbed by the reactor, which should match the enthalpy change of the chemical reaction $\dot{n}\, DH_{rxn}$ per unit time. The incoming solar power is determined by the normal beam insolation I, by the collector area, and by taking into account the optical imperfections of the collection system (e.g., reflectivity, specularity, tracking imperfections). The capability of the collection system to concentrate solar energy is often expressed in terms of its mean flux concentration ratio $\tilde{C}$ over an aperture normalized with respect to the incident normal beam insolation as follows:

$$\tilde{C} = \frac{Q_{aperture}}{I A_{aperture}}\,. \qquad (5)$$

For simplification, we assume an aperture size that captures all incoming power so that $Q_{aperture} = Q_{solar}$. With this assumption and for a perfectly insulated isothermal blackbody cavity-receiver ($a_{eff}=e_{eff}=1$), Eqs. (4) and (5) are combined to yield

$$h_{absorption} = 1 - \left(\frac{s T^4}{I\tilde{C}} \right). \qquad (6)$$

The absorbed concentrated solar radiation drives an endothermic chemical reaction. The measure of how well solar energy was converted into chemical energy for a given process is the exergy efficiency, defined as

$$h_{exergy} = \frac{-\dot{n} DG_{rxn}\big|_{298K}}{Q_{solar}} \quad , \qquad (7)$$

where DG_{rxn} is the maximum possible amount of work that may be extracted from the products as they are transformed back to reactants at 298 K. The 2nd law is now applied to calculate the maximum exergy efficiency $h_{exergy,ideal}$. Since the conversion of solar process heat to DG_{rxn} is limited by both the solar absorption and Carnot efficiencies, the maximum overall efficiency is

$$h_{exergy,ideal} = h_{absorption} \times h_{Carnot} = \left[1 - \left(\frac{s T_H^4}{\tilde{IC}}\right)\right] \times \left[1 - \left(\frac{T_L}{T_H}\right)\right] \qquad (8)$$

where T_H and T_L are the upper and lower operating temperatures of the equivalent Carnot heat engine. $h_{exergy,ideal}$ is plotted in Fig. 6 as a function of T_H for T_L = 298 K and for various solar flux concentrations.

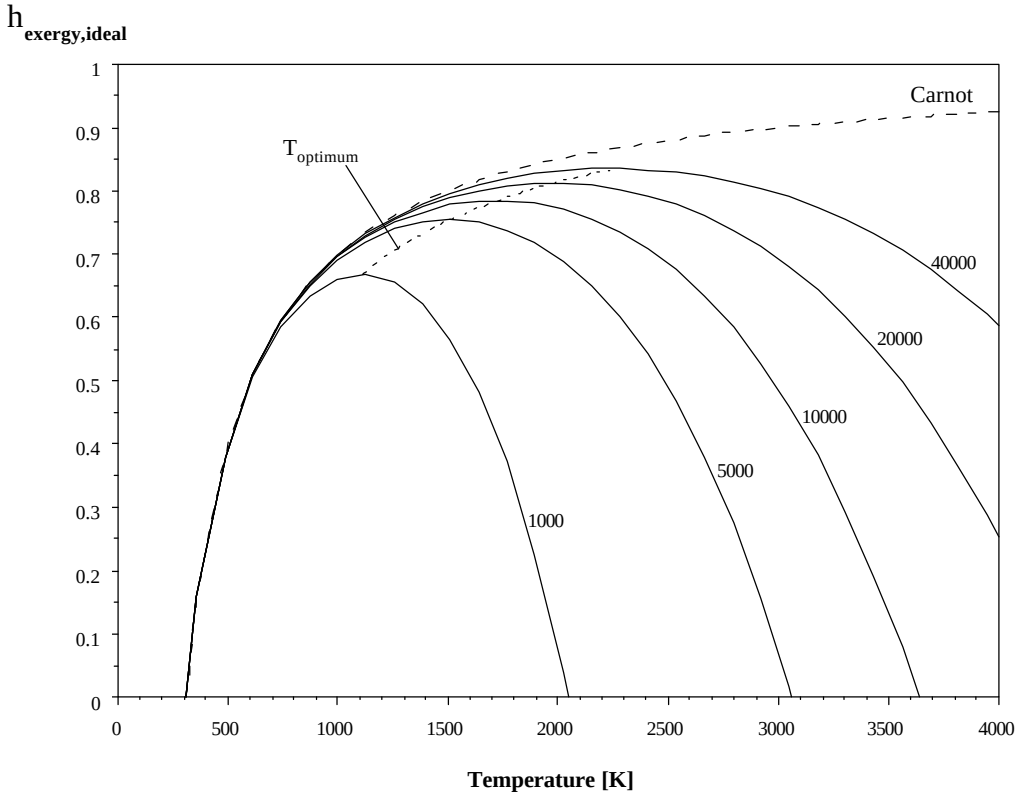

Figure 6. The ideal exergy efficiency $h_{exergy,ideal}$ is shown as a function of the operating temperature T_H, for a blackbody cavity-receiver converting concentrated solar energy into chemical energy [Eq. (8); T_L = 298 K]. The mean solar flux concentration is the parameter: 1000, 5000, ...40000. Also plotted is the Carnot efficiency and the locus of the optimum cavity temperature $T_{optimum}$ (Eq. 11).

Because of the Carnot limit, one should try to operate thermochemical processes at the highest upper temperature possible; however, from a heat-transfer perspective, the higher the temperature, the higher the re-radiation losses. The highest temperature an ideal solar cavity-receiver is capable of achieving, defined as the stagnation temperature $T_{stagnation}$, is calculated by setting $h_{exergy,ideal}$ equal to zero, which yields

$$T_{stagnation} = \left(\frac{\tilde{IC}}{s}\right)^{0.25} \quad . \qquad (9)$$

At this temperature, $h_{exergy,ideal}$ = 0 because energy is being re-radiated as fast as it is absorbed. Concentration ratios of 10,000 and more have been achieved using paraboloidal primary reflectors and non-imaging secondary concentrators (such as CPCs), which translate to stagnation temperatures above 3600 K. However, an energy-efficient process must run at temperatures that are substantially below $T_{stagnation}$. There is an optimum temperature $T_{optimum}$ for maximum efficiency obtained by setting

$$\frac{\partial h_{exergy,ideal}}{\partial T} = 0 \quad . \qquad (10)$$

Assuming a uniform power-flux distribution, this relation yields the following implicit equation for $T_{optimum}$:

$$T_{optimum}^5 - (0.75T_L)T_{optimum}^4 - \left(\frac{a_{eff}T_L I\tilde{C}}{4e_{eff}s}\right) = 0 \quad . \quad (11)$$

Equation (11) was solved numerically (Steinfeld and Schubnell, 1993) and the locus of $T_{optimum}$ is shown in Fig. 6. The optimal temperature for maximum efficiency varies between 1100 and 1800 K for uniform power-flux distributions with concentrations between 1000 and 13,000. For example, when $\tilde{C}$ = 2000 and I = 900 W/m^2, the maximum efficiency corresponds to about 1250 K. For a Gaussian incident power-flux distribution having peak concentration ratios between 1000 and 12,000 suns, the optimal temperature varies from 800 to 1300 K. In practice, when considering convection and conduction losses in addition to radiation losses, the efficiency will peak at a somewhat lower temperature.

The pertinent questions that follow from the preceding arguments are the following: (1) What are the best chemical systems for solar thermochemical processing? (2) What are the optimum temperatures for these processes? One criterion for making comparative judgments of various solar processes is the ideal exergy efficiency [see Eq. (7)]. To help apply this term, one can think of solar processes that lead to fuels as ideal cyclic processes like that shown in Fig. 7, which uses a solar reactor, a quenching device, and a fuel cell.

The complete process is carried out at constant pressure. In practice, pressure drops will occur throughout the system. If one assumes, however, frictionless operating conditions, no pumping work is required. The reactants may be pre-heated in an adiabatic heat exchanger where some portion of the sensible and latent heat of the products is transferred to the reactants; for simplicity, a heat exchanger has been omitted. The reactor is assumed to be a perfect blackbody cavity-receiver. The reactants enter the solar reactor at T_L and are further heated to the reactor temperature T_H. Chemical equilibrium is assumed inside the reactor. The net power absorbed in the solar reactor should match the enthalpy change per unit time of the reaction,

$$Q_{reactor,net} = \dot{n}DH\big|_{Reactants@T_L \rightarrow Products@T_H} \quad (12)$$

Irreversibilites in the solar reactor arise from the non-reversible chemical transformation and re-radiation losses to the surroundings at T_L. It is found that

$$Irr_{reactor} = \left(\frac{-Q_{solar}}{T_H}\right) + \left(\frac{Q_{rerad}}{T_L}\right) + \left(\dot{n}DS\big|_{Reactants@T_L \rightarrow Products@T_H}\right) . \quad (13)$$

Products exit the solar reactor at T_H and are cooled rapidly to T_L. The amount of power lost during quenching is

$$Q_{quench} = -\dot{n}DH\big|_{Products@T_H \rightarrow Products@T_L} . \quad (14)$$

The irreversibility associated with quenching is

$$Irr_{quench} = \left(\frac{Q_{quench}}{T_L}\right) + \left(\dot{n}DS\big|_{Products@T_H \rightarrow Products@T_L}\right) \quad (15)$$

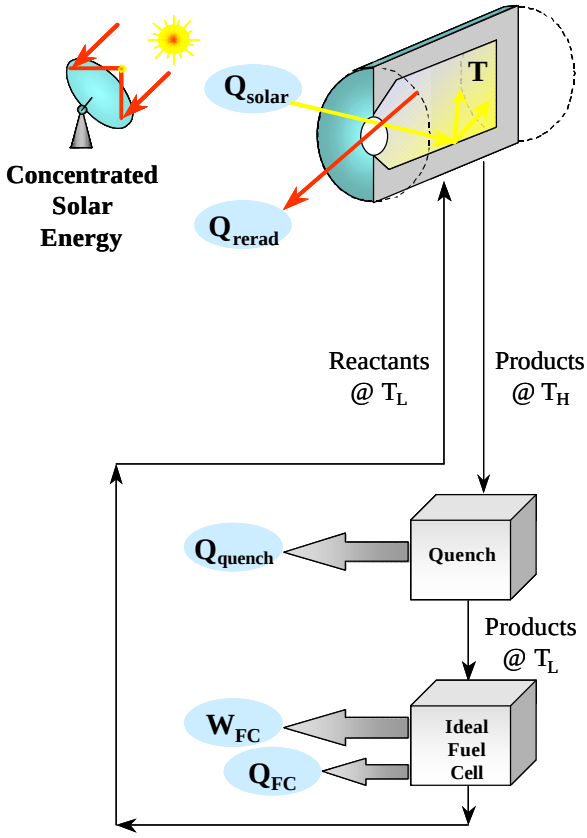

Figure 7. Schematic of an ideal cyclic process for calculating the maximum exergy efficiency of a solar thermochemical process.

The cycle is closed by introducing a reversible, ideal fuel cell, in which the products recombine to form the original reactants and thereby generate electrical power in the amount

$$W_{FC} = \dot{n}DG\big|_{Products@T_L \rightarrow Reactants@T_L} . \quad (16)$$

W_{FC} is the maximum amount of work that the products leaving the reactor could produce if they combined at

T_L and a total pressure of 1 bar. This work value is also known as the exergy of the products at ambient temperature. The fuel cell operates isothermally; where the amount of heat rejected to the surroundings is

$$Q_{FC} = -T_L \times \dot{n} DS\big|_{Products@T_L \rightarrow Reactants@T_L} \cdot (17)$$

The exergy system efficiency of the closed-cycle is then calculated using Eq. (7) as

$$h_{exergy} = \frac{W_{FC}}{Q_{solar}} \cdot \qquad (18)$$

Check – This thermodynamic analysis is verified by performing an energy balance and by evaluating the maximum achievable efficiency (Carnot efficiency) from the total available work and from the total power input. The energy balance confirms that

$$W_{FC} = Q_{solar} - (Q_{rerad} + Q_{quench} + Q_{FC}) . (19)$$

The available work is calculated as the sum of the fuel-cell work plus the lost work due to irreversibilities in the solar reactor and during quenching. Thus,

$$h_{max} = \frac{W_{FC} + T_L \cdot (Irr_{reactor} + Irr_{quench})}{Q_{solar}} \cdot (20)$$

This maximum efficiency must be equal to that of a Carnot heat engine operating between T_H and T_L , i.e.

$$h_{max} = h_{Carnot} = 1 - \frac{T_L}{T_H} \cdot \qquad (21)$$

Example: The ZnO/Zn-Cycle

In order to illustrate the use of equations (1)-(21), we consider as an example a solar process in which the following chemical transformation occurs

$$ZnO(s)\big|_{298K} \rightarrow Zn(s) + \frac{1}{2} O_2\Big|_{298K} \qquad (22)$$

The variations of $DH°_{rxn}$, $DG°_{rxn}$, and $TDS_{rxn}°$ for reaction (22) with temperature are shown in Fig. 8. At 2235 K, $DG°_{rxn} = 0$. Above 2235 K, $DG°_{rxn} < 0$ and the reaction proceeds spontaneously to the right by supplying $DH°_{rxn}$ solar process heat. Table 1 gives a numerical description for the components shown in Fig. 7 for the ZnO thermal dissociation as an example of how one evaluates the exergy efficiency of a process as well as how one quantifies the intrinsic entropy production of the process. The analysis of this particular system is relatively simple. The reader is referred to Steinfeld *et al* (1996) for a more complex system. This kind of process modeling establishes a base for evaluating and comparing different solar thermochemical processes for ideal, closed cyclic systems that recycle all materials and also for open systems that allow for material flow into and out of the system.

Table I. Exergy analysis of the solar thermal dissociation of ZnO using the process modeling depicted in Fig. 7. The ZnO molar rate $\dot{n}$ is assumed 1 mol/s.

Assumptions	T_L = 298 K, T_H = 2300 K, p=1 bar, C=5000, $\dot{n}$ =1 mol/s
Q_{solar}	815 kW
Q_{rerad}	258 kW
$Q_{reactor,net}$	557 kW
$Irr_{reactor}$	0.81 kW/K
Q_{quench}	209 kW
Irr_{quench}	0.52 kWK
Q_{FC}	30 kW
W_{FC}	318 kW
$h_{absorption}$	68 %
h_{Carnot}	87 %
$h_{exergy,ideal}$	59 %
h_{exergy}	39 %

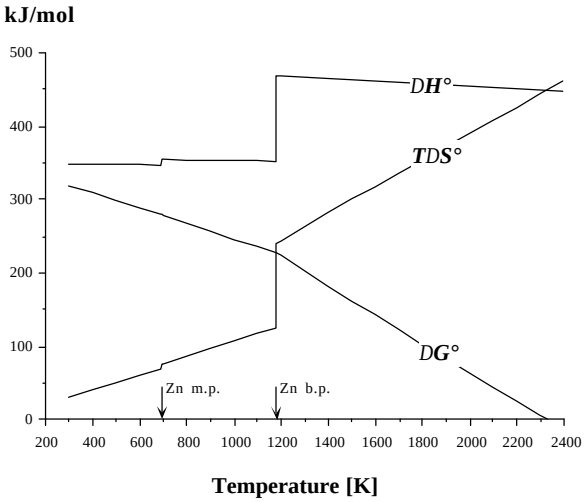

Figure 8. Energy requirements for *ZnO(s) ® Zn + 0.5 O_2*.

All solar thermal chemical processes can be thought of in this manner, and their exergy efficiencies can be compared as one criterion for judging their relative industrial potential. The higher the exergy efficiency, the lower is the required solar collection area for producing a given amount of solar fuel and, consequently, the lower are the costs incurred for the solar concentrating system, which usually correspond to half of the total investments for the entire solar chemical plant. Thus, high exergy efficiency implies favorable competitiveness. It is important to note that we have a thermal cycle receiving thermal energy from a high-temperature reservoir and rejecting it to a low-

temperature reservoir. If we pick a chemical system where everything in the cycle could be done perfectly, the maximum efficiency would be the Carnot efficiency. Thus, the higher the temperature at which one supplies process heat, the more work-like and thus the more valuable the process heat. But there is an important caveat. A Carnot cycle is one where there are no internal sources of entropy-production. When entropy is produced one looses some capacity for doing useful work. Examples of common entropy production mechanisms are friction, heat transfer across temperature differences, and most chemical reactions. The moment one selects a specific solar process, one inherits the intrinsic process entropy-production mechanisms. Some processes have higher exergy efficiencies than others, and any individual process has some preferred operating temperature. Furthermore, the entropy production calculations guide one's thinking in creating process ideas. The lost work calculations tell the solar process designer the potentially most thermodynamically profitable places for creating new concepts. In the above example, the quench can reduce the process efficiency by as much as 33%. The lost-work calculation suggests finding an alternative method for separating the products. This fact was the impetus for research into electrolytic methods for separating the gas phase products at high temperatures.

One will recognize that thermodynamics is a powerful tool used in the field of solar thermochemistry. But it does not tell the entire story with regard to the potential performance of a solar process. Specifically, it does not give insight into the rates of the chemical reactions. It is beyond the scope of this review to go into much detail on the importance of chemical kinetics in the field of solar thermochemistry. Understanding the complex interactions between solar flux, reactant feed conditions, and chemical kinetics is important for designing reactors that convert solar energy efficiently into chemical fuels. Low activation energy to favor kinetics, large enthalpy change to maximize energy-conversion capacity, and small molar volume of products to minimize handling/storage volume are some of the general guidelines for the selection of solar chemical processes.

IV. SOLAR THERMOCHEMICAL PROCESSES

IV.1. Solar Hydrogen: The Direct Thermal Dissociation of H_2O

Some of the earliest work in solar thermochemistry was dedicated to the direct thermal dissociation of water, also known as thermolysis of water, i.e.

$$H_2O \rightarrow H_2 + \tfrac{1}{2} O_2 \qquad (23)$$

The processes investigated to date used a zirconia surface, solar-heated to temperatures of or above 2500 K, and subjected to a stream of water vapor. The gaseous products that result from the water thermolysis need to be separated at high-temperatures to avoid recombination or ending with an explosive mixture. Among the ideas proposed for separating the H_2 from the products are effusion separation (Fletcher and Moen, 1977; Kogan, 1998), and electrolytic separation (Ihara, 1980; Fletcher, 1999). Rapid quench by injecting a cold gas or by expansion in a nozzle, followed by a low-temperature separation, are simpler and workable (Diver *et al.*, 1983; Lédé *et al.*, 1987), but the quench introduces a significant drop in the exergy efficiency of the process. Furthermore, the very high temperatures demanded by the thermodynamics of the process pose severe material problems and can lead to significant re-radiation from the reactor, thereby lowing the absorption efficiency and, consequently, further lowing the exergy efficiency. These obstacles pushed research in the direction of water-splitting thermochemical cycles (*see Section IV.5*).

IV.2. Solar Hydrogen: Thermal Decomposition of H_2S

Several papers describe solar chemical processes for producing H_2 and S_2 by thermally decomposing H_2S, from which this discussion is extracted (Noring and Fletcher, 1982; Kappauf *et al.*, 1985; Kappauf and Fletcher, 1989; Harvey *et al.*, 1998; Diver and Fletcher, 1985). H_2S is a highly toxic industrial product recovered in large quantities in the sweetening of natural gas and in the removal of organically bound sulfur from petroleum and coal. Current industrial practice uses the Claus process to recover the sulfur from H_2S, but the process wastes H_2 by oxidizing it to H_2O to produce low-grade process heat. In 1979, the amount wasted in the US and Canada alone amounted to the equivalent of 17 million barrels of gasoline. Furthermore it has been pointed out that some natural gas wells throughout the world are so rich in H_2S that they are not used. A solar process that converted the highly toxic material into a useful fuel would make a substantial contribution to the world's energy pipeline. In one such process, H_2S is fed to a solar thermal chemical reactor operating at temperatures near 1800 K and pressures between 0.03- 0.5 bar. At these operating conditions, the sulfide is cracked into H_2 and S on a hot Al_2O_3 surface, viz.,

$$H_2S \rightarrow H_2 + \tfrac{1}{2} S_2 \qquad (24)$$

The product gas mixture is quenched at the exit of the reactor in a water-cooled heat exchanger,

producing liquid and ultimately solid sulfur and thereby separating the H_2 from the S_2. Experimental evidence suggests that the quench is relatively easy; the reverse reaction between the products seems to be unimportant at temperatures as high as 1500 K. A recent study delineating the chemical kinetics of the decomposition reaction gives a quantitative rate expression for H_2S decomposing in an alumina reactor in the temperature range of 1350 - 1600 K. (Harvey *et al.*, 1998). An economic analysis indicates that, assuming H_2S has zero value (this is a conservative choice) and a price for electric energy of $0.05/kWh, the solar thermal decomposition of H_2S could have a pay-back time as short as 6.3 years (Diver and Fletcher, 1985).

IV.3. Solar Chemical Heat Pipes

Solar chemical heat pipe refers to the solar energy conversion concept depicted in Fig. 9. High-temperature solar process heat is used for driving an endothermic reversible reaction in a solar chemical reactor. The products can be stored long-term and transported long-range to the customer site where the energy is needed. At that site, the exothermic reverse reaction is effected, yielding process heat in an amount equal to the stored solar energy $DH_{A®B}$. This high-temperature heat may be applied for example to generate electricity using a Rankine cycle. The chemical products for the reverse reaction are the original chemicals; they are returned to the solar reactor and the process is repeated. Two reverse reactions that have been extensively investigated for application in chemical heat pipes are the CH_4 reforming-methanation and the NH_3 dissociation-synthesis.

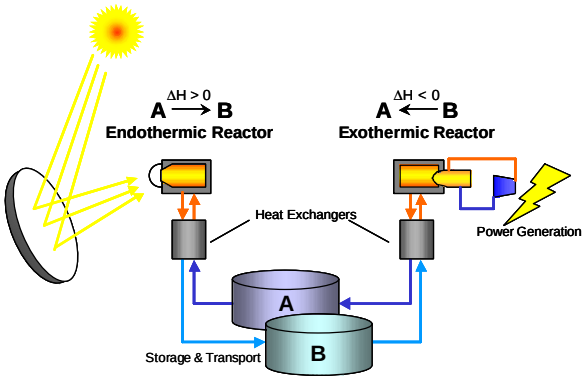

Figure 9. Solar chemical heat pipe for the storage and transportation of solar energy. High-temperature solar process heat is used to drive the endothermic reversible reaction *A®B*. The product *B* may be long-term stored and long-range transported to the site where the energy is needed. At that site, the exothermic reverse reaction *B®A* is effected and yields high-temperature process heat in an amount equal to the stored solar energy $DH_{A®B}$. The chemical product of the reverse reaction *A* is returned to the solar reactor for reuse.

Methane undergoes reforming to synthesis gas (syngas), a mixture of primarily H_2 and CO, when using either H_2O or CO_2 as the partial oxidizing agent as follows

$$CH_4 + H_2O \leftrightarrow 3H_2 + CO \qquad (25)$$

$$CH_4 + CO_2 \leftrightarrow 2H_2 + 2CO \qquad (26)$$

Reactions (25) and (26) are endothermic by 206 and 247 kJ/mol, respectively, and proceed catalytically above 1100 K. Reaction (26) has been studied in solar furnaces with small-scale solar reactor prototypes using an Rh-based catalyst (Levy *et al.*, 1992; Muir *at al.*, 1994), and recently scaled-up to power levels of 300 - 500 kW in a solar tower facility using a high-pressure (8-10 bar) tubular reactor and a low-pressure (1-3 bar) volumetric reactor (Epstein and Spiewak, 1996; Abele *et al.*, 1996).

The dissociation of ammonia

$$NH_3 \leftrightarrow \frac{3}{2}H_2 + \frac{1}{2}N_2 \qquad (27)$$

is endothermic by 70 kJ/mol and proceeds catalytically at high-pressures (50-200 bar) and at temperatures above 700 K. It is being investigated for application in a distributed-dish concentrating system with the reverse synthesis reaction delivering heat to a Rankine cycle. A techno-economic feasibility study for a 10-MW power-plant design, with a net solar-to-electric conversion efficiency of 18% and a capacity factor of 80%, indicates a levelized energy cost of 0.16 US$1999 per kWh (Lovegrove *et al.*, 1999, Luzzi *et al.*, 1999).

IV.4. Solar Thermal, Electrothermal, and Carbothermal Reduction of Metal Oxides

Metals are attractive candidates for storage and transport of solar energy. They may be used to generate either high-temperature heat via combustion or electricity via fuel cells and batteries. Metals can also be used to produce hydrogen via a water-splitting reaction; the hydrogen may be further processed for heat and electricity generation. The chemical products from any of these power-generating processes are metal oxides which, in turn, need to be reduced and recycled. The conventional extraction of metals from their oxides by carbothermic and electrolytic processes is characterized by its high energy consumption and its concomitant environmental pollution. The extractive metallurgical industry discharges vast amounts of greenhouse gases and other pollutants to the environment, derived mainly from the combustion of fossil fuels for heat and electricity generation. These emissions can be substantially reduced, or even completely eliminated, by using concentrated solar energy as the source of high-T process heat.

The thermal and electrothermal reduction of metal oxides without using a reducing agent and the carbothermal reduction of metal oxides using C(gr) and CH_4 as reducing agents may be represented as follows:

$$M_xO_y \rightarrow xM + \frac{y}{2}O_2 \quad (28)$$

$$M_xO_y + yC(gr) \rightarrow xM + yCO \quad (29)$$

$$M_xO_y + yCH_4 \rightarrow xM + y(2H_2 + CO) \quad (30)$$

where M denotes the metal and M_xO_y the corresponding metal oxide. The Gibbs free energy of formation of many stable metallic oxides such as ZnO, MgO, SiO_2, CaO, Al_2O_3, and TiO_2 are large negative numbers that decrease in magnitude with temperature, while their enthalpy of formation remains relatively independent of temperature. The variation of the energy requirement for the thermal and electrothermal dissociation of these metal oxides with temperature is depicted in Fig. 5 for a generic solar chemical reaction, and in Fig. 8 for the thermal dissociation of ZnO. Table II lists the approximate temperatures at which the standard $DG°_{rxn}$ for reactions (28), (29), and (30) equals 0 for various metal oxides of interest (JANAF, 1985; Steinfeld *et al.*, 1998a).

The solar thermal dissociation of ZnO is among the most promising metal oxide processes. A simplified exergy analysis for this process has been presented in *Section III*. A kinetic study reported an apparent activation energy in the range 310-350 kJ/mole (Hirschwald and Stolze, 1972, Palumbo *et al.*, 1998). The product gases need to be quenched to avoid re-oxidation, which introduces irreversibilities and may be a factor of complexity in large-scale utilization. In particular, the quench efficiency is sensitive to the dilution ratio of zinc and oxygen in an inert gas flow and to the temperature of the surface on which the products are quenched. Maximum exergy efficiencies exceeding 50% are possible for a molar ratio of an inert gas to ZnO(s) less than 1 (Palumbo *et al.*, 1998). The condensation of Zn(g) in the presence of O_2 was studied by fractional crystallization in a temperature-gradient tube furnace. The oxidation of Zn is a heterogeneous process and, in the absence of nucleation sites, Zn(g) and O_2 can coexist in a meta-stable state (Weidenkaff *et al.*, 1999).

Except for the thermal dissociation of ZnO, the required temperature for effecting reaction (28) exceeds 3500 K. Although it is possible to attain such stagnation temperatures with high-flux solar concentrating systems that deliver concentration ratios above 10,000 [see Eq. (9)], practical engineering and heat-transfer considerations suggest operation of solar reactors at substantially lower temperatures, especially when the process is to be conducted with high energy absorption efficiency [see Eq. (6)]. Under these circumstances, solar process heat alone will not make the reaction proceed; some amount of high-quality energy is required in the form of work. It may be supplied in the form of electrical energy in electrolytic processes or in the form of chemical energy by introducing a reducing agent in thermochemical processes.

Table II. Approximate temperatures for which $DG°_{rxn}$ of reactions (28), (29), and (30) equals zero.

Metal Oxide	$DG°_{rxn28}=0$ @	$DG°_{rxn29}=0$ @	$DG°_{rxn30}=0$ @
Fe_2O_3*	3700 K	920 K	890 K
Al_2O_3	> 4000 K	2320 K	1770 K
MgO	3700 K	2130 K	1770 K
ZnO	2335 K	1220 K	1110 K
TiO_2*	> 4000 K	2040 K	1570 K
SiO_2*	4500 K	1950 K	1520 K
CaO	4400 K	2440 K	1970 K

*Fe_2O_3, TiO_2, and SiO_2 decompose to lower-valence oxides before complete dissociation to the metal.

An example of a solar electrothermal reduction process that has been demonstrated experimentally in a solar furnace is the electrolysis of ZnO. As shown in Fig. 8, at 1000 K up to 30% of the total amount of energy required to produce Zn could be supplied by solar process heat. In such an electrochemical process, an electrolytic cell is housed in a solar cavity receiver that is irradiated with concentrated solar energy. ZnO(s) is dissolved into an electrolyte composed of a combination of sodium, aluminum and/or calcium fluoride with a melting point near the process temperature. This choice prevents excess loss of electrolyte due to evaporation. Electric energy is then supplied to two electrodes immersed in a saturated solution. If the electrodes are made of graphite, the products are essentially CO and Zn (Fletcher *et al.*, 1985, Fletcher, 1999). If the anode is made of Pt and the cathode is made of Mo the products are Zn and O_2 (Palumbo and Fletcher, 1988). ZnO(s) can also be dissociated thermally in a cell. The O_2 is then separated from the Zn vapor by pumping it electrolytically through a cell wall made of zirconia sandwiched between two Pt surfaces (Parks *et al.*, 1988). Solar electrochemistry research in this field has to date been almost exclusively dedicated to ZnO and H_2O, but one can extend the thinking to the high-temperature electrolysis or

quasi-electrolysis of MgO, Al_2O_3, and other interesting candidate materials (Fletcher, 1999).

If one wishes to decompose metal oxides thermally into their elements without the application of electrical work, a chemical reducing agent is necessary to lower the dissociation temperature. Coal as coke and natural gas as methane are preferred reducing agents in blast-furnace processes because of their availability and relatively low price. In the presence of carbon, the uptake of oxygen by the formation of CO brings about reduction of the oxides at much lower temperatures. While reactions (29) and (30) have favorable free energies above the temperatures indicated in Table II, a more detailed calculation of the chemical equilibrium composition shows that only the carbothermic reduction of Fe_2O_3, ZnO, and MgO will result in significant free metal formation below about 2000 K. The carbides TiC, SiC, Al_3C_4, and CaC_2 are thermodynamically stable in an inert atmosphere; the nitrides TiN, Si_3N_4, and AlN are stable in N_2 atmosphere. Examples of carbothermic reduction processes that have been carried out in solar furnaces include the production of Fe, Mg, and Zn from their metal oxides in Ar atmospheres, the production of AlN, TiN, Si_3N_4, and ZrN from their metal oxides in N_2 atmospheres, and the production of Al_4C_3, TiC, SiC, and CaC_2 from their metal oxides in Ar atmospheres (Steinfeld and Fletcher, 1991; Murray *et al.*, 1995; Duncan and Dirksen, 1980).

Using natural gas as a reducing agent combines in a single process the reduction of metal oxides with the reforming of methane for the co-production of metals and synthesis gas (syngas), [see Eq. (30)]. The resulting syngas mixture has a molar ratio of H_2 to CO equal to 2, which makes it especially suitable for methanol synthesis. Since the evolved product gases are sufficiently valuable commodities to justify their collection, discharge of gaseous reaction products to the environment is eliminated. Thermal reductions of Fe_3O_4 and ZnO with CH_4 to produce Fe, Zn, and syngas have been demonstrated in solar furnaces using fluidized bed and vortex type reactors (Steinfeld *et al.*, 1993; Steinfeld *et al.*, 1995; Steinfeld *et al.*, 1998b). These reactions are endothermic by 333 kJ/mol Fe and 442 kJ/mol Zn, respectively, and proceed to completion at temperatures above about 1250 K.

IV.5. Solar Hydrogen: H_2O-splitting thermochemical cycles

Single-step (direct) thermal water dissociation, although conceptually simple, has been impeded by the need to use very high temperatures and an effective technique for separating H_2 and O_2. Water-splitting thermochemical cycles have been proposed to bypass the H_2/O_2 separation problem. Multi-step thermochemical cycles also allow the use of relatively moderate operating upper temperatures, but their overall exergy efficiency is limited by irreversibilities associated with heat transfer and product separation. A status review on multi-step cycles was given in 1992 by Serpone *et al.* and includes a 3-step cycle based on the solar decomposition of H_2SO_4 at 1140 K and a 4-step cycle based on the solar hydrolysis of $CaBr_2$ and $FeBr_2$ at 1020 K and 870 K, respectively. Two-step water-splitting cycles, based on metal oxides redox systems, require much higher temperatures, but, when using high solar concentration ratios and heat-recovery systems, have the potential of achieving efficiencies above 30% (Steinfeld *et al.*, 1998a). The first, endothermic step is the solar thermal dissociation of metal oxides [see Eq. (28) in *Section IV.4*]. The second, non-solar, exothermic step is the hydrolysis of the metal at moderate temperatures (below about 800 K) to form molecular hydrogen and the corresponding metal oxide, i.e.

$$xM + yH_2O \rightarrow M_xO_y + yH_2 \qquad (31)$$

The products have a natural phase separation. The liberated heat may be used to effect the reaction in an auto-thermal reactor. This 2-step solar thermochemical cycle is shown schematically in Fig. 10. The net reaction is $H_2O \rightarrow H_2 + 0.5O_2$. Hydrogen and oxygen are formed in different steps, thereby eliminating the need for high-temperature gas separation.

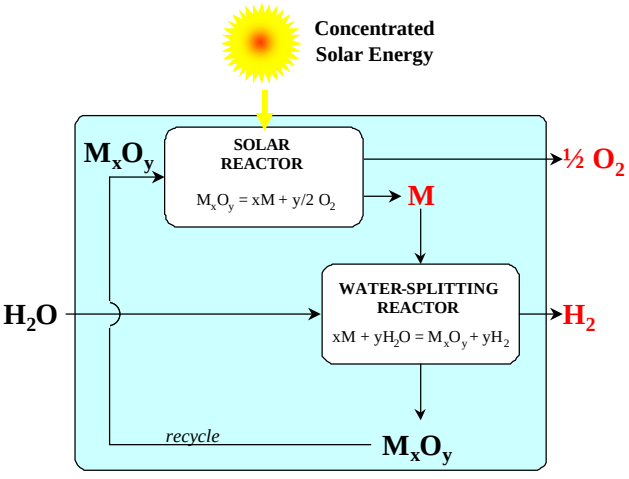

Figure 10. Schematic of a two-step water-splitting thermochemical cycle using metal oxides in redox systems. In the first, endothermic, solar step, the metal oxide M_xO_y is thermally decomposed into the metal M and oxygen. Concentrated solar radiation is the energy source for the required high-temperature process heat. In the second, exothermic, non-solar step, the metal M reacts with water to produce hydrogen. The resulting metal oxide is then recycled back to the first step. The net reaction is $H_2O \rightarrow H_2 + 0.5\ O_2$. Since hydrogen and oxygen are produced in different steps, the need for high temperature gas separation is eliminated.

In some cases, a lower-valence metal oxide is capable of splitting water, so that complete reduction of the metal oxide to the metal is not necessary. These cycles have been examined thermodynamically and tested in solar reactors for ZnO/Zn and Fe_3O_4/FeO redox pairs (Bilgen *et al.* 1977; Nakamura, 1977; Palumbo *et al.*, 1998; Sibieude *et al.*, 1982; Steinfeld *et al.*, 1998a; Steinfeld *et al.*, 1999). Other redox pairs, such as TiO_2/TiO_x, Mn_3O_4/MnO, and Co_3O_4/CoO have also been considered, but the yield of H_2 in reaction (31) has been too low to be of any practical interest. Partial substitution of iron in Fe_3O_4 by other metals forms mixed metal oxides of the type $(Fe_{1-x}M_x)_3O_4$ that may be reducible at lower temperatures than those required for the reduction of Fe_3O_4, while the reduced phase $(Fe_{1-x}M_x)_{1-y}O$ remains capable of splitting water (Ehrensberger *et al.*, 1995).

IV.6. Solar Upgrade and Decarbonization of Fossil Fuels

The replacement of fossil fuels by solar fuels, e.g., solar hydrogen and solar metals, is a long-term goal. It requires the development of novel technologies and it will take time before these methods are technically and economically ready for commercial applications. Thus, from a strategic point of view, it is desirable to consider a mid-term goal that aims at the development of hybrid solar/fossil processes. Any endothermic process that uses fossil fuels exclusively as chemical reactants and solar energy as the source of process heat qualifies as an hybrid solar/fossil process. The products are fuels whose quality has been upgraded by solar energy, i.e. the calorific value is increased above that of the fossil fuel by solar energy input equal to the enthalpy change of the reaction. Increased energy content means extended fuel life and reduced pollution of the environment. Therefore, these fuels are *cleaner* fuels. The mix of solar and fossil energies creates a link between current fossil-fuel-based technologies and future solar chemical technologies. This approach builds bridges between present and future energy economies. Solar technologies will represent viable economic paths earlier if the costs of fossil energy account properly for environmental externalities arising from the burning of fossil fuels. The transition from fossil to solar fuels can occur smoothly, and the lead time for transferring important solar technology to industry can be reduced. Figure 11 illustrates the research strategy which is aimed at both the long-term goal of using solar fuels and at the mid-term goal of applying solar-fossil fuel mixtures.

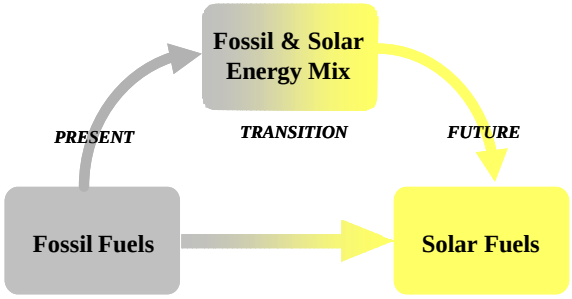

Figure 11. Strategy for replacement of fossil fuels by solar fuels, which involves research on two paths: a long-term path for a completely sustainable energy supply, and a mid-term path for mixing fossil and solar energies.

Examples of processes involving mixed fossil and solar energies are the carbothermic reduction of metal oxides using coke or natural gas as chemical reducing agents. Use of these types of processes will substantially reduce greenhouse-gas emissions. For example, a life cycle analysis indicates that replacing conventional fossil-fuel-based zinc production by a solar-based CH_4-thermal reduction process results in CO_2-equivalent emission reductions of 59% (Werder and Steinfeld, 2000).

Another important category of thermochemical processes for mixing fossil and solar energies is the decarbonization of fossil fuels, i.e. the removal of carbon from fossil fuels prior to their combustion so that no CO_2 is discharged during combustion. Two methods have been considered (Steinberg, 1999): (1) the solar thermal decomposition of fossil fuels and (2) the steam-reforming/gasification of fossil fuels. The thermal decomposition of natural gas, oil, and other hydrocarbons may represented by

$$C_xH_y \rightarrow xC(gr) + \frac{y}{2}H_2 \quad . \qquad (32)$$

Other compounds may also be formed, depending on the reaction kinetics and the presence of impurities in the raw materials. But the thermal decomposition yields basically two distinct products that have a natural phase separation, namely, a carbon-rich condensed phase and a hydrogen-rich gas phase. The carbonaceous solids can either be sequestered or used as material commodities under less severe CO_2 constraints. The hydrogen-rich gas mixtures may be further processed to high-purity hydrogen that is not contaminated by carbon oxides and that can be used in fuel cells without inhibiting the use of platinum-made electrodes. H_2-rich mixtures can also be adjusted to yield high-quality syngas.

The steam-reforming of natural gas, oil, and other hydrocarbons is represented by

$$C_xH_y + xH_2O \rightarrow \left(\frac{y}{2} + x\right)H_2 + xCO \qquad (33)$$

and the steam-gasification of coal by

$$coal + H_2O \rightarrow H_2, CO \qquad (34)$$

As in thermal decompositions, other compounds may also be formed, especially from coal. Some impurities contained in the raw materials such as sulfur compounds are removed prior to decarbonization by using conventional technologies. The principal product is syngas of different H_2:CO mole ratios. The CO content in the syngas may be shifted toward H_2 via the catalytic water-gas shift reaction

$$CO + H_2O \rightarrow H_2 + CO_2 \qquad (35)$$

CO_2 is separated from H_2, for example, by pressure swing adsorption (PSA).

Reactions (32) to (34) proceed endothermically in the 800-1500 K range. Several chemical aspects of these reactions have already been studied (Ullmann, 1996). Reaction (32) has been effected catalytically by using solar process heat at about 823 K for the production of filamentous carbon (Meier *et al.*, 1999). Reaction (33) has been demonstrated in a solar tower using natural gas (*see Section IV.3*) and is currently being considered for the use of low petroleum gas (a gas mixture that results from petroleum distillation containing mainly propane and butane) using the same reactor technology (Epstein and Spiewak, 1996; Abele *et al.*, 1996). Reaction (34) has also been performed using solar energy in early exploratory studies, for example, with oil shale (Ingel *et al.*, 1992, Fletcher and Berber, 1988). Some of these processes are currently practiced at an industrial scale and the energy required for heating of the reactants and for the heat of reaction is supplied by burning some portion of the feedstock. As an example, to crack methane according to Eq. (32), at least 20% of the higher heating value of the feedstock is used. For methane reforming according to Eq. (33), about 40% of the feedstock needs to be burned to supply process heat. Internal combustion results in contamination of the gaseous products while external combustion results in reduced thermal efficiency because of the irreversibilities associated with indirect heat transfer via heat exchangers. The use of solar energy for process heat has the following advantages: (1) the discharge of pollutants is avoided; (2) gaseous products are not contaminated; and (3) the calorific value of the fuel is upgraded by adding solar energy in an amount equal to the *DH* of the reaction.

The two solar thermal decarbonization methods are shown schematically in Fig. 12 in the form of simplified process flow diagrams.

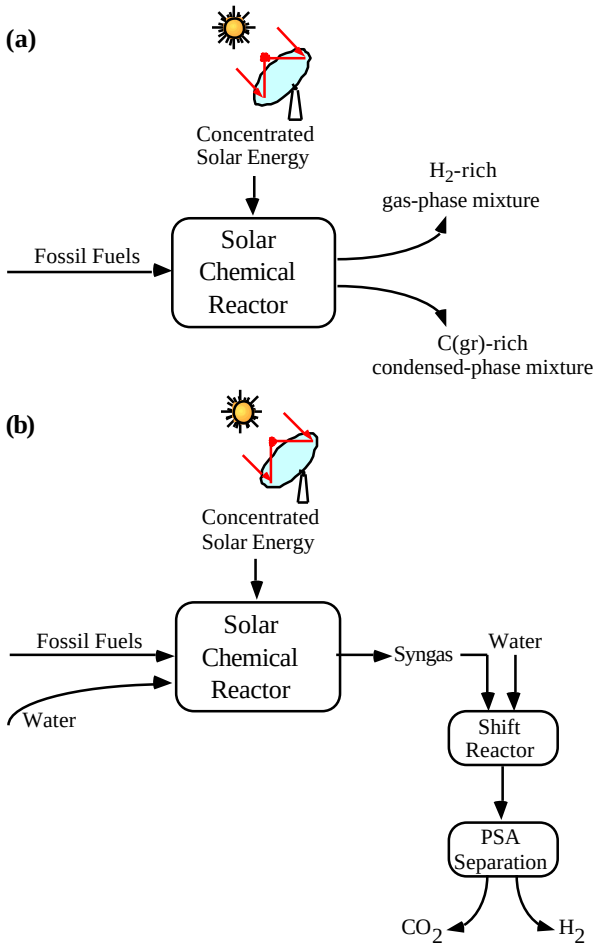

Figure 12. Simplified process flow diagram for the solar thermal decarbonization of fossil fuels. Two methods are considered: (a) solar thermal decomposition and (b) solar thermal steam-reforming/gasification. Omitted are the formation of by-products derived from impurities present in the feedstock and the pre-treatment of the fossil fuels (e.g., by desulfurization).

The two methods have been compared (Steinberg, 1999). From the point of view of carbon sequestration, it is easier to separate, handle, transport and store solid carbon than gaseous CO_2. The steam-reforming/gasification method requires additional steps for shifting CO and separating CO_2, while thermal decomposition accomplishes the removal and separation of carbon in a single step. In contrast, the major drawback of the thermal decomposition method is the energy loss associated with the sequestration of carbon. For this approach, the type of feedstock is of crucial importance when selecting the decarbonization method. For example, thermal decomposition may be the preferred option for gaseous hydrocarbons because of the high H_2/C ratio. But for coal and other solid carbonaceous materials, the residual of energy after decarbonization may be too low for industrial application. Gasification of coal via reaction (34) has the additional advantage of converting a relatively dirty solid fuel, which is traditionally used to generate electricity in steam-turbine cycles at about

35% efficiency, into a cleaner fluid fuel when using solar process heat that can be used in gas-turbine or combined cycles with over 55% efficiency.

Many fossil fuel reserves exist in regions with high solar insolation. Thermochemical processes that mix fossil fuels with solar energy, such as those described here, are important intermediate solutions towards a sustainable energy-supply system.

IV.7. Solar thermal production of chemical commodities

Concentrated solar energy may be used for the processing of high-temperature and energy-intensive commodities. Examples are the following. (a) Syngas may be produced by solar reforming or solar gasification of fossil fuels according to Eqs. (33) and (34) (*see Section IV.6*). Syngas is the building block for a wide variety of synthetic fuels, including Fischer-Tropsch type chemicals, hydrogen, ammonia, and methanol (which is a possible substitute for gasoline in vehicles). (b) Biomass and other carbonaceous materials may be converted in different solar thermochemical routes into bio-oils, charcoal, and syngas (Lédé, 1999). A significant advantage of using biomass is that the process has a zero net release of CO_2. (c) Fullerenes and carbon nanotubes can be produced by sublimation of C(graphite) above 3000 K or by catalytic thermal decomposition of hydrocarbons according to Eq. (32), (Guillard *et al.*, 1999; Meier *et al.*, 1999). (d) Metallic carbides and nitrides can be produced by the solar carbothermic reduction of metal oxides as in Eqs. (29) and (30), (*see Section IV.4*). These ceramics are valuable materials for high-temperature applications because of their high hardness, excellent corrosion resistance, high melting points, and low coefficients of thermal expansion. They may also be incorporated in cyclic processes of the type shown in Fig. 10; their hydrolysis yields hydrocarbons and ammonia (Murray *et al.*, 1995). (e) Zinc, iron, magnesium, and other metals can be produced by the carbothermic reduction of their metal oxides (*see Section IV.4*). Aluminum-silicon alloys may be produced by the carbothermic reduction of Al_2O_3 and SiO_2 at 2300 K, thus providing an alternative route to the Hall-Héroult electrolytic process (Murray, 1999). (f) Decomposition of limestone, the main endothermic step in the production of cement, may be effected using solar process heat at 1300 K.

IV.8. Solar thermal detoxification and recycling of waste materials

Solid waste materials from a wide variety of sources (e.g., municipal waste incineration residuals, discharged batteries, dirty scraps, contaminated soil, dusts and sludge, and other by-products from the metallurgical industry) contain hazardous compounds that should not be discharged into the environment. They are usually vitrified in a non-leaching slag and finally disposed of at hazardous waste-storage sites. However, limited storage space, increasing storage costs, and environmental regulations have led to the urgent need of developing technologies that recycle these toxic materials into useful commodities rather than deposit them in dump sites for an undetermined period of time. Chemical transformations of these materials into their elemental components offers the possibility of converting waste materials into valuable feedstock for processes in closed materials cycles. Thermal processes are well suited for the treatment of complex solid waste materials. Waste materials containing carbonaceous compounds can be converted by thermal pyrolysis and gasification into syngas and hydrocarbons that can be further processed into other valuable synthetic chemicals. Waste materials containing metal oxides may be converted by carbothermal reduction into metals, nitrides, carbides, and other metallic compounds. The chemical products from such transformations are feedstock for a variety of manufacturing processes and may also be used as fuels.

Closed cycles of materials require high-temperature, energy-intensive recycling processes. The commercial recycling techniques by blast, induction, arc, and plasma furnaces are major consumers of electricity and high-temperature process heat and, consequently, major contributors of greenhouse-gas emissions and other pollutants. Concentrated solar radiation supplies clean thermal energy at high temperatures to drive these complex processes that usually involve gases, solids, and melts. Preliminary feasibility tests with aluminium melts were conducted in a solar furnace with a rotary-kiln solar reactor (Funken *et al.*, 1999).

V. SOLAR THERMOCHEMICAL REACTORS

The chemical thermodynamics and kinetics of the reaction place important constrains on the size, type, materials of construction, and modes of operation of reactors. The species involved and their phases, temperature requirements, enthalpies, and rates of reaction are among essential information required for reactor design. The design of a multi-purpose reactor that optimizes every reaction is an impossible task. However, reactors may be classified according to general types that will guide their designs. They may be reactors for homogeneous and heterogeneous chemical systems, for batch, semi-batch and steady-flow operations, for plug or mixed flows, etc. We refer the reader to the introductory book of Levenspiel (1992) for a comprehensive treatment on chemical reactor engineering.

A unique feature of solar chemical reactors is that the source of process heat is concentrated solar energy. Therefore, the heat transfer characteristics of a solar reactor may differ significantly from those existing in conventional designs. We have found it useful to classify solar reactors into two groups: (i) Indirectly-irradiated reactors, i.e. reactors in which the opaque external walls of the reactor are exposed to concentrated solar radiation and transfer the absorbed heat to the chemical reactants. (ii) Directly-irradiated reactors, i.e. reactors in which the chemical reactants (or catalysts) are directly exposed to the concentrated solar radiation.

There are benefits and drawbacks associated with both concepts. Indirectly-irradiated reactors have the advantage of eliminating the need for a transparent window. Disadvantages are linked to limitations imposed by the materials of construction of the reactor walls such as the maximum operating temperature, thermal conductivity, radiative absorptance, inertness, resistance to thermal shocks, and suitability for transient operation. Directly-irradiated reactors have the advantage of providing efficient radiation heat transfer directly to the reaction site where the energy is needed and thereby by-passing the aforementioned limitations imposed by indirect heat transport through the reactor walls. Furthermore, under proper conditions, direct irradiation may enhance photochemical kinetics. The major drawback, when working with reducing or inert atmospheres, is the requirement for a transparent window, which is a critical and troublesome component in high-pressure and severe gas environments. Both directly- and indirectly-irradiated reactors suffer intrinsic losses in energy conversion efficiency as the result of re-radiation losses. Since these losses are proportional to the re-radiation area, they can be minimized by using cavity-type solar receivers.

A solar cavity-type receiver is basically a well-insulated enclosure designed to capture effectively the incident solar radiation by allowing entry of radiation only through a small opening [the *aperture* (*see Section III*)]. Because of multiple internal reflections, the fraction of the incoming energy absorbed by the cavity greatly exceeds the simple surface absorptance of the inner walls. This effect is called the cavity effect and may be expressed as an apparent absorptance which is defined as the fraction of energy flux emitted by a blackbody surface stretched across the cavity opening that is absorbed by the cavity walls. The apparent absorptance has been calculated for cylindrical, conical and spherical geometries having diffuse and specularly reflecting inner walls (Siegel and Howell, 1972). The larger the ratio of the cavity diameter or depth to the aperture diameter, the closer the cavity-receiver approaches a blackbody absorber. Smaller apertures also serve to reduce re-radiation losses. However, they intercept a reduced fraction of the sunlight reflected from the concentrators. Consequently, the optimum aperture size is a compromise between maximizing radiation capture and minimizing radiation losses. The optimum aperture radius $r_{optimum}$ for a Gaussian power flux distribution according to $F_{peak} \times exp(-r^2/2m^2)$, where F_{peak} is the peak solar flux intensity at $r=0$ and m denotes the radius corresponding to one standard deviation for the power flux distribution, is (Steinfeld and Schubnell, 1993)

$$r_{optimum} = \left[-2m^2 \, ln\left(\frac{sT^4}{F_{peak}} \right) \right]^{0.5} \quad . \qquad (36)$$

The optimal aperture radius varies from 2.6 to $2.9m$ for peak solar flux intensities between 1,000 and 12,000 suns.

The following is an example of a directly-irradiated solar chemical reactor for high-temperature solid-gas processes (Haueter *et al.*, 2000). Other examples of solar chemical reactor for various thermochemical applications may be found in the cited literature. Figure 13 is a detailed schematic of a directly-irradiated reactor concept designed for the solar thermal dissociation of ZnO(s) into Zn(g) and O_2 at temperatures above 2000 K [Eq. (22), *see Section III*].

It is a reactor closed to air. The main component is a rotating conical cavity-receiver (#1) made of inconel steel that contains the aperture (#2) for access of concentrated solar radiation through a quartz window (#3). Because of multiple reflections at the inner walls of the cavity, the cavity approaches a blackbody absorber that captures and absorbs incoming solar energy efficiently. The solar flux

concentration may be further augmented by incorporating (*see Section II*) a CPC (#4) in front of the aperture. Both the copper-made window mount and the aluminum-made CPC are water-cooled and integrated into a concentric (non-rotating) conical shell (#5). The reactants are ZnO particles which are fed continuously along the axis into the rotating cavity by means of a screw powder feeder located at the rear of the reactor (#6). The centripetal acceleration forces the ZnO powder to the wall where it forms a thick layer of ZnO (#7) that insulates and reduces the thermal load on the inner cavity walls. The gaseous products Zn and O_2 are swept out of the chamber by a continuous flow of inert gas that enters the cavity-receiver tangentially at the front (#8) and exits via an outlet port (#9) to a quench device (#10). The purge gas also keeps the window cool and clear of particles or condensable gases.

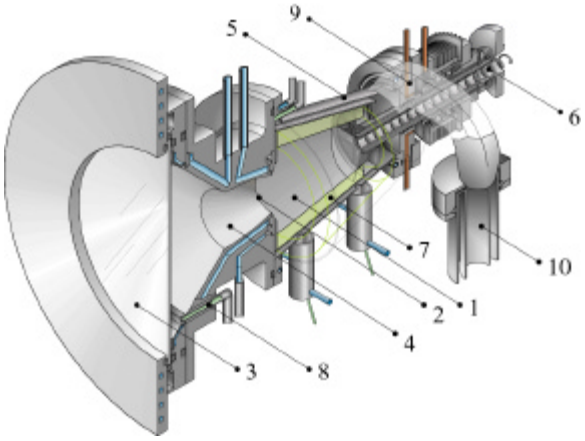

Figure 13. Schematic of a solar chemical reactor for the thermal decomposition of ZnO [Eq. (22)]. 1= rotating cavity-receiver, 2 = aperture, 3 = quartz window, 4 = CPC, 5 = outside conical shell, 6 = reactant feeder, 7 = ZnO layer, 8 = purge-gas inlet, 9 = product outlet port, 10 = quench device.

With this arrangement, concentrated sunlight impinges directly on the top surface of the ZnO layer. This efficient heating condition leads to a system with a low thermal inertia and excellent thermal shock resistance. The ZnO serves simultaneously as radiation absorber, thermal insulator, and chemical reactant. An indirectly-irradiated version of this reactor may be obtained by incorporating a graphite cavity at the aperture. Concentrated solar radiation is then absorbed by the cavity and further transferred to the reactants by combined conduction, convection, and radiation heat transfer.

Other directly-irradiated reactor concepts have been demonstrated experimentally with gas-particle suspensions, fluidized beds, perforated graphite disks, ceramic honeycombs and foams, and other radiation absorbers for transferring heat to reactants and/or catalysts (Kappauf *et al.*, 1985; Ingel *et al.*, 1992; Levy *et al.*, 1992; Abele *et al.*, 1996, Muir *at al.*, 1994; Steinfeld *et al.*, 1998b). Most of these solar experiments were performed with small-scale prototype reactors at an early stage of R&D. Especially the window technology requires further development and feasibility demonstration at a larger scale. In contrast, the indirectly-irradiated reactor concept uses well-established engineering practices and has already been demonstrated at 0.5 MW for a tubular solar reformer operating at 1100 K (Epstein and Spiewak, 1996). For large-scale applications at moderate temperatures, it may be preferable over the near term to apply the indirectly-irradiated concept for the reactor design. Over the long term, directly-irradiated reactors for advanced applications at temperatures exceeding 1500 K may prove to have superior performance.

VI. OUTLOOK

After the 1973/74 Middle East oil crisis, the world community began to appreciate its dependence on a precarious supply of crude oil. The International Energy Agency was created to help ensure the development of cheap and stable energy-resource options. The agency's objectives continue to makes sense. It has been pointed out that a country's national security and control of its own political destiny depend on access to energy. Unfortunately, access to conventional sources of energy for a nation are not secure and could be cut off. Whether it be a war, depletion of a major energy source such as crude oil, or a threat to the environment such as the greenhouse effect, these are sound reasons for countries to invest in the development of energy options. From this perspective, solar energy research is "preventive medicine for the health of a country" (Fletcher, 1996).

This view leads to a profound change in the role of economics in guiding research. Rather than evaluating solar chemistry technology options by how well they compete economically against conventional fossil-fuel-based technologies in the current market place, economic arguments would challenge new sustainable energy technology options to be more economical than the best current ones. If the goal were to produce H_2, the economic competition should properly be between sustainable concepts for producing it. If solar energy is to be used to reduce CO_2 emissions, the solar process should be more cost effective than all other options

that bring atmospheric CO_2 levels to sustainable values.

If solar thermochemical or other renewable energy technologies for producing fuels and chemical commodities are required to compete with all other production technologies, the cost of fossil-fuel-based materials and processes involved in those technologies must be forced to account for the externalities of burning fossil fuels such as the cost of CO_2 mitigation and pollution abatement. These external costs may be assessed by conducting a life cycle analysis (LCA) which is a method for evaluating the environmental burdens associated with a product, process, or activity by identifying and quantifying energy and materials used and wastes released to the environment during the entire life cycle. When the external costs are internalized, renewable energy technologies may well become competitive with conventional technologies.

Solar-made electricity is a key form of clean energy based on an unlimited resource, but it cannot be stored or transmitted over long distances more conveniently than electricity produced from any other energy sources. Solar-made chemical fuels overcome these limitations to a large extent. They are solar energy carriers that can be used for heat and electricity generation to match the customer's energy demands. Solar thermochemical processes are thermodynamically favorable paths for producing solar fuels because of the potential for converting unlimited solar energy into chemical energy efficiently. Thus, solar thermochemical process technology is a promising long-term prospect for delivering clean, efficient, sustainable energy services.

VII. REFERENCES

Abele, M., Woerner, A., Brose, G., Buck, R., and Tamme, R. (1996). Test results of a receiver-reactor for solar methane reforming and aspects of further application of this technology. *In Proceedings of the 8th Int. Symp. Solar Thermal Concentrating Technologies*, 6-11 October, 1996, Cologne, Germany, pp. 1185-1204, Müller Verlag, Heidelberg.

Bilgen, E., Ducarroir, M., Foex, M., Sibieude, F., and Trombe, F. (1977). Use of solar energy for direct and two-step water decomposition cycles. *Int. J. Hydrogen Energy* **2**, 251- 257.

Diver, R.B., and Fletcher, E. A. (1985). Hydrogen and Sulfur From H_2S — III. The Economics of a Quench Process. *Energy* **10**, 831-842.

Diver, R. B., Pederson, S., Kappauf, T., and Fletcher, E. A. (1983). Hydrogen and Oxygen from Water — VI. Quenching the Effluent from a Solar Furnace. *Energy* **12**, 947-955.

Duncan, D. A., and Dirksen, H. A. (1980). Calcium Carbide Production in a Solar Furnace. SERI/TR-98326-1, Golden, CO, USA.

Epstein, M., and Spiewak, I. (1996). Solar Experiments with a Tubular Reformer. *In Proceedings of the 8th Int. Symp. Solar Thermal Concentrating Technologies*, 6-11 October, 1996, Cologne, Germany, pp. 1209-1229, Müller Verlag, Heidelberg.

Ehrensberger, K., Frei, A., Kuhn, P., Oswald, H. R., and Hug, P. (1995). Comparative experimental investigations on the water-splitting reaction with iron oxide $Fe_{1-y}O$ and iron manganese oxides $(Fe_{1-x}Mn_x)_{1-y}O$. *Solid State Ionics* **78**, 151-160.

Fletcher, E. A. (1996). Solar thermochemical and electrochemical research—How they can help reduce the carbon dioxide burden. *Energy* **21**, 739-745.

Fletcher, E. A. (1999). Solarthermal and solar quasi-electrolytic processing and separations: Zinc from Zinc Oxide as an example. *Ind. Eng. Chem. Res*. **38**, 2275-2282.

Fletcher, E. A., and Berber, R. (1988). Extracting Oil from Shale Using Solar Energy. *Energy* **13**, 13-23.

Fletcher, E. A., Macdonald, F., and Kunnerth, D. (1985). High temperature solar electrothermal processing II. Zinc from zinc oxide. *Energy* **10**, 1255-1272.

Fletcher, E. A, and Moen, R. L.(1977). Hydrogen and Oxygen From Water. *Science* **197**, 1050-1056.

Funken, K.-H., Pohlmann, B., Lüpfert, E., and Dominik, R. (1999). Application of concentrated solar radiation to high temperature detoxification and recycling processes of hazardous wastes. *Solar Energy* **65**, 25-31.

Guillard, T., Alvarez, L., Anglaret, E., Sauvajol, J. L., Bernier, P., Flamant, G., and Lapalze, D. (1999). Production of fullerenes and carbon nanotubes by the solar energy route, *J. Phys. IV France* **9**. 399-404.

Harvey, S., Davidson, Jane, H., and Fletcher, E. A. (1998). Thermolysis of Hydrogen Sulfide in the Temperature Range 1350 to 1600 K. *Ind. Eng. Chem. Res.* **37**, 2323-2332.

Haueter, P., Moeller, S., Palumbo, R., and Steinfeld, A. (2000). The Production of Zinc by Thermal Dissociation of Zinc Oxide – Solar Chemical Reactor Design. *Solar Energy*, in press.

Haueter, P., Seitz, T., and Steinfeld, A. (1999). A New High-Flux Solar Furnace for High-Temperature Thermochemical Research. *J. Solar Energy Engineering* **121**, 77-80, 1999.

Hirschwald, W., and Stolze, F. (1972). Kinetics of the Thermal Dissociation of Zinc Oxide. *Zeitschrift für Physikalische Chemie Neue Folge* **77,** 21-42.

Ingel, G., Levy, M., and Gordon, J. (1992). Oil shale gasification by concentrated sunlight: an open-loop solar chemical heat pipe. *Energy* **17**, 1189-1197.

Ihara, S. (1980). On the study of hydrogen production from water using solar thermal energy. *Int. J. Hydrogen Energy* **5**, 527-534.

JANAF Thermochemical Tables (1985). National Bureau of Standards, 3rd ed., Washington, D.C..

Kappauf, T., and Fletcher, E. A. (1989). Hydrogen and Sulfur from Hydrogen Sulfide — VI. Solar Thermolysis. *Energy* **14**, 443-449.

Kappauf, T., Murray, J. P., Palumbo, R. Diver, R. B., and Fletcher, E. A. (1985). Hydrogen and Sulfur from Hydrogen Sulfide — IV. Quenching the Effluent from a Solar Furnace. *Energy* **10**, 1119-1137.

Kogan, A. (1998). Direct solar thermal splitting of water and on-site separation of the products. II. Experimental feasibility study. *Int. J. Hydrogen Energy* **23**, 89-98.

Lédé, J. (1999). Solar thermochemical conversion of biomass. *Solar Energy* **65**, 3-13.

Lédé, J., Villermaux, J., Ouzane, R., Hossain, M. A., and Ouahes, R. (1987). Production of hydrogen by simple impingement of a turbulent jet of steam upon a high temperature zirconia surface. *Int. J. Hydrogen Energy* **12**, pp. 3-11.

Levenspiel, O. (1972). *Chemical Reaction Engineering*. 2nd edition, John Wiley & Sons, Inc., New York.

Levy, M., Rubin, R., Rosin, H., and Levitan, R. (1992), Methane Reforming by Direct Solar Irradiation of the Catalyst. *Solar Energy* **17**, 749-756.

Lovegrove, K., Luzzi, A., McCann, M., and Freitag, O. (1999) Exergy analysis of ammonia-based thermochemical solar power systems. *Solar Energy* **66**, 103-115.

Luzzi, A., Lovegrove, K., Filippi, E., Fricker, H., Schmitz-Goeb, M., and Chandapillai, M. (1999). Base-load solar thermal power using thermochemical energy storage. *J. Phys. IV France* **9**, 105-110.

Meier, A., Kirillov, V., Kuvshinov, G., Mogilnykh, Y., Reller, A., Steinfeld, A., and Weidenkaff, A. (1999). Solar Thermal Decomposition of Hydrocarbons and Carbon Monoxide for the Production of Catalytic Filamentous Carbon. *Chemical Engineering Science* **54**, 3341-3348.

Muir, J., Hogan, R., Skocypec, R., and Buck, R. (1994). Solar Reforming of methane in a direct absorption catalytic reactor on a parabolic dish: I. Test and Analysis. *Solar Energy* **52**, 467-477.

Murray, J. P. (1999). Aluminum-Silicon Carbo-thermal Reduction Using High-Temperature Solar Process Heat. *Light Metals*, Eckert C. E. (ed), pp. 399-405. The Minerals, Metals, and Materials Society, Warrendale, PA

Murray, J. P., Steinfeld, A., and Fletcher E. A. (1995). Metals, Nitrides, and Carbides Via Solar Carbothermal Reduction of Metals Oxides. *Energy* **20**, 695-704.

Nakamura, T. (1977). Hydrogen production from water utilizing solar heat at high temperatures. *Solar Energy* **19**, 467-475.

Noring, J. E., and Fletcher, E. A. (1982). High Temperature Solar Thermochemical Processing — Hydrogen and Sulfur from Hydrogen Sulfide. *Energy* **7**, 651-666.

Palumbo, R. D., and Fletcher, E. A. (1988). High temperature solar electro-thermal processing III. Zinc from zinc oxide at 1200-1675 K using a non-consumable anode. *Energy* **13**, 319-332.

Palumbo, R., Lédé, J., Boutin, O., Elorza Ricart, E., Steinfeld, A., Möller, S., Weidenkaff, A., Fletcher, E. A., and Bielicki, J. (1998). The Production of Zn from ZnO in a Single Step High Temperature Solar Decomposition Process. *Chemical Engineering Science* **53**, 2503-2518.

Parks, D. J., Scholl, K. L., and Fletcher, E. A. (1988). A study of the use of Y_2O_3 doped ZrO_2 membranes for solar electrothermal and solar thermal separations. *Energy* **13**, 121-136.

Serpone, N., Lawless, D., and Terzian, R. (1992). Solar Fuels: Status and Perspectives. *Solar Energy* **49**, 221-234.

Sibieude, F., Ducarroir, M., Tofighi, A., and Ambriz, J. (1982). High-Temperature Experiments with a Solar Furnace: the Decomposition of Fe_3O_4, Mn_3O_4, CdO. *Int. J. Hydrogen Energy* **7**, 79-88.

Siegel, R., and Howell, J.R. (1992). *Thermal Radiation Heat Transfer*. 3rd Ed., Hemisphere Publishing Corporation, Washington D.C.

SolarPACES (1996). *Solar Thermal Test Facilities*, Editorial CIEMAT, Madrid.

Steinberg, M. (1999). Fossil fuel decarbonization technology for mitigating global warming. *Int. J. Hydrogen Energy* **24**, 771-777.

Steinfeld, A., Brack, M., Meier, A., Weidenkaff, A.,and Wuillemin, D. (1998b). A Solar Chemical Reactor for the Co-Production of Zinc and Synthesis Gas. *Energy* **23**, 803-814.

Steinfeld, A., and Fletcher, E. A. (1991). Theoretical and Experimental Investigation of the Carbothermic Reduction of Fe_2O_3 Using Solar Energy. *Energy* **16**, 1011-1019.

Steinfeld, A., Frei, A., Kuhn, P., and Wuillemin, D. (1995). Solarthermal Production of Zinc and Syngas Via Combined ZnO-Reduction and CH_4-Reforming Processes. *Int. J. Hydrogen Energy* **20**, 793-804.

Steinfeld, A., Kuhn, P., and Karni, J. (1993). High Temperature Solar Thermochemistry: Production of Iron and Synthesis Gas by Fe_3O_4-Reduction with Methane. *Energy* **18**, 239-249.

Steinfeld, A., Kuhn, P., Reller, A., Palumbo, R., Murray, J., and Tamaura, Y. (1998a). Solar-Processed Metals as Clean Energy Carriers and Water-Splitters. *Int. J. Hydrogen Energy* **23**, 767-774.

Steinfeld, A., Larson, C., Palumbo, R., and Foley M. (1996). Thermodynamic Analysis of the Co-Production of Zinc and Synthesis Gas Using Solar Process Heat. *Energy* **21**, 205-222.

Steinfeld, A., Sanders, S., and Palumbo, R. (1999). Design Aspects of Solar Thermochemical Engineering. *Solar Energy* **65**, 43-53.

Steinfeld, A., and Schubnell, M. (1993). Optimum Aperture Size and Operating Temperature of a Solar Cavity-Receiver. *Solar Energy* **50**, 19-25.

Tyner, C. E., Kolb, G. J., Meinecke, W., Trieb F. (1999). Concentrating Solar Power in 1999 – An IEA/SolarPACES Summary of Status and Future Prospects. SolarPACES 1999.

Ullmann's Encyclopedia of Industrial Chemistry (1996). 5th Edition, B. Elvers, S. Hawkins, Editors, VCH Verlagsgesellschaft: Weinheim, Germany.

Weidenkaff, A., Steinfeld, A., Wokaun, A., Eichler, B., and Reller, A. (1999). The Direct Solar Thermal Dissociation of ZnO: Condensation and Crystallisation of Zinc in the Presence of Oxygen. *Solar Energy* **65**, 59-69.

Welford, W. T., and Winston, R. (1989). *High Collection Nonimaging Optics*, Academic Press, San Diego, USA.

Werder, M., and Steinfeld, A. (2000). Life Cycle Assessment of the Conventional and Solarthermal Production of Zinc and Synthesis Gas. *Energy*, **25**, 395-409.

Yogev, A., Kribus, A., Epstein, M., and Kogan, A. (1998). Solar Tower Reflector Systems: A New Approach for High-Temperature Solar Plants. *Int. J. Hydrogen Energy* **23**, 239-245.